Nordic Journal of Surveying and Real Estate Research 10:1 (2014) 63–79
submitted on 22 April, 2013
revised on 4 September, 2013
accepted on 2 October, 2013

Cycle Slip Detection in Single Frequency GPS Carrier Phase Observations Using Expected Doppler Shift

Peter Cederholm, **Darius Plausinaitis**
Aalborg University
Department of Development and Planning
Denmark
pce@land.aau.dk, dpl@plan.aau.dk

Abstract. *The article presents a case study of cycle slips detection in double differenced L1 carrier phase observations collected with two low–cost single frequency GPS receivers operating in both static and kinematic mode. The receivers deliver half–cycle carrier phase observations. Cycle slips are identified using expected Doppler shift. Expected Doppler shift is computed from the positions and the velocities of the satellites and the receivers.*

A static and a kinematic experiment are carried out. In the static experiment both GPS receivers are stationary while data are collected, whereas one receiver is mounted on a moving car in the kinematic experiment.

In the static experiment, cycle slips with a magnitude of 0.5 cycle are easily detected. In this case the positions of the receivers are estimated from collected code observations, and the velocities of the receivers are zeros as they are stationary.

In the kinematic experiment, the positions of the receivers are again estimated from code observations, and the velocities of the receivers are estimated from collected Doppler shift observations. The accuracy of the estimated velocities is so poor that the expected Doppler shift does not make it possible to detect cycle slips with a magnitude of 0.5 cycle. Cycle slips must have magnitudes of several cycles in order to be safely identified.

Computer simulations indicate that the velocities should have a standard deviations of 0.05 m/s or less in order to detect 0.5 cycle slips.

Key words. *Cycle slip detection, Doppler shift, ublox ANTARIS 4 LEA-4T, DGPS.*

1 Introduction

Relative GPS positioning using carrier phase observations from two receivers is capable of producing a vector between the two receivers with a precision of a few centimetres or better. This level of precision is only achievable if cycle slips in the collected carrier phase observations have been correctly identified and accounted for. A cycle slip is a jump in the accumulated carrier phase observation by an integer number of cycles. Three sources of cycle slips are identified by (Hofmann-Wellenhof et al., 2008), p. 195. The first source is physical obstructions that block the signal. The second source is low signal to noise ratio, and the third source is failure in the receiver software. Many techniques for identifying cycle slips have been presented over the years. Some of these techniques are outlined in (Xu, 2003), pp. 151–153 and (Hofmann-Wellenhof et al., 2008), pp. 194–202. Some techniques require dual frequency observations whereas other techniques only need single frequency observations. In general, it is more difficult to detect cycle slips in single frequency observations than it is in dual frequency observations. The paper focuses on a single frequency technique.

One of the techniques that only requires single frequency observations is Doppler integration that uses observed Doppler shift to predict the growth in the carrier phase observations from one epoch to the next. A deviation between the predicted and the observed carrier phase observation may indicate a cycle slip. However, the noise level of the observed Doppler shift is often high, which makes this technique inadequate for identifying small cycle slips (Liu, 2010), p. 172. To remedy this problem, this article suggests using expected Doppler shift rather than observed Doppler shift for detecting cycle slips. The expected Doppler shift can be computed once the relative receiver–satellite motion is known. Satellite positions and velocities are computed from the ephemerides. Receiver positions and velocities are computed from collected code observations and Doppler shift observations.

The article presents a case study in which observations from two low–cost single frequency ublox ANTARIS 4 LEA-4T GPS receivers are used for illustrating the favorable and less favorable aspects of using expected Doppler shifts for detecting cycle slips. The receivers collect half-cycle carrier phase observations. The case study includes observations collected in both static and kinematic mode. One of the receivers (*master*) is always static. The other receiver (*rover*) is stationary in static mode and moving in kinematic mode. When operating in static mode, cycle slips with a magnitude of 0.5 cycle are easily detected. When operating in kinematic mode, cycle slips cannot be identified unless they have a magnitude of several cycles. The reason for the latter is that it is not possible to estimate the rover receiver velocity with sufficient accuracy (Lipp and Gu, 1994), p. 683. Simulations based on the collected observations and computer generated white gaussian noise suggest that the rover receiver velocity should have a standard deviation of 0.05 m/s or less in order to successfully detect 0.5 cycle slips.

The article is divided into seven parts. Part one is this introduction. Part two presents how cycle slips are identified using Doppler shift. Part three presents observed and expected Doppler shifts, respectively. Part four describes the conducted experiment. Part five and six present the results of the experiment and the simulations. Part seven presents the conclusions of the research.

2 Cycle slip detection using Doppler shift

The frequency of the received GPS signal differs from the frequency of the transmitted signal. This difference in frequency, which is partly caused by the relative motion of the satellite and the receiver is named the Doppler shift. The Doppler shift (Δf) is the radial component of the relative receiver–satellite velocity vector (seen form the receiver) divided by the transmitted wavelength (Misra and Enge, 2001), p. 16.

$$\Delta f = \frac{v_{radial}}{\lambda}, \tag{1}$$

where v_{radial} is the relative radial velocity vector, and λ is the transmitted wavelength.

Doppler shifts can be used to detect cycle slips in carrier phase observations between neighbouring epochs. The carrier phase observation at one epoch is predicted based on the Doppler shift and the carrier phase observation from the previous epoch. The predicted carrier phase observation is (Cannon et al., 1992), p. 4

$$\Phi_A^j(t+1) = \Phi_A^j(t) + \frac{\Delta f_A^j(t+1) + \Delta f_A^j(t)}{2}\,\Delta t, \tag{2}$$

- ▷ where $\Phi_A^j(t+1)$ is the predicted carrier phase observation from satellite j to receiver A at epoch $(t+1)$,
- ▷ $\Phi_A^j(t)$ is the carrier phase observation at epoch (t),
- ▷ $f_A^j(t+1)$ and $f_A^j(t)$ are the Doppler shifts at epoch $(t+1)$ and epoch (t) respectively, and finally
- ▷ Δt is the time span between epoch $(t+1)$ and epoch (t).

If the predicted carrier phase observation and the actual observed carrier phase observation at epoch $(t+1)$ do not agree within a certain tolerance, a cycle slip may have occurred. As an alternative to equation (2), (Mertikas and Rizos, 1997), p. 471 suggest another way of estimating the predicted carrier phase observation which is more robust

$$\Phi_A^j(t+1) = \Phi_A^j(t) + \sqrt{\Delta f_A^j(t+1) \cdot \Delta f_A^j(t)}\,\Delta t. \tag{3}$$

Equation (2) and to some extent equation (3) assume a constant change in Doppler shifts over Δt. This assumption holds for static applications and for short time spans. When this assumption is violated by long time spams and/or by the

receiver moving, the predicted carrier phase observations will be less precise rendering the cycle slip detection less efficient. The threshold for deciding whether a deviation between an observed and a predicted carrier phase observation should be identified as a cycle slip depends on the precision of the Doppler shift, the receiver dynamics, and the magnitude of Δt.

Equations (2) and (3) predict a single carrier phase observation from satellite j to receiver A. However, relative carrier phase positioning between two receivers is most often based on double differenced carrier phase observations. The double differenced (*DD*) carrier phase observation between receivers A and B and satellites j and k is (Hofmann-Wellenhof et al., 2008), p. 176

$$\Phi_{AB}^{jk}(t) = \Phi_B^k(t) - \Phi_B^j(t) - \Phi_A^k(t) + \Phi_A^j(t). \tag{4}$$

Instead of predicting a single carrier phase observation equations (2) and (3) can be expanded to predict a double differenced carrier phase observation. First, a double differenced Doppler shift observation at epoch (t) between the two receivers and the two satellites is computed

$$\Delta f_{AB}^{jk}(t) = \Delta f_B^k(t) - \Delta f_B^j(t) - \Delta f_A^k(t) + \Delta f_A^j(t). \tag{5}$$

A similar double differenced Doppler shift observation is computed at epoch $(t+1)$. Now, it is possible to predict the double differenced carrier phase observation using either

$$\Phi_{AB}^{jk}(t+1) = \Phi_{AB}^{jk}(t) + \frac{\Delta f_{AB}^{jk}(t+1) + \Delta f_{AB}^{jk}(t)}{2}\,\Delta t, \tag{6}$$

or the more robust alternative

$$\Phi_{AB}^{jk}(t+1) = \Phi_{AB}^{jk}(t) + \sqrt{\Delta f_{AB}^{jk}(t+1) \cdot \Delta f_{AB}^{jk}(t)}\,\Delta t. \tag{7}$$

The noise level of $\Phi_{AB}^{jk}(t)$ is a few millimetres (Cederholm, 2010). Therefore, the noise level of the predicted double differenced carrier phase observation $\Phi_{AB}^{jk}(t+1)$ largely depends on the noise level of the double differenced Doppler shift observations.

3 Observed and expected Doppler shifts

Equations (2) and (3) can either be used with observed Doppler shifts or expected Doppler shifts. Observed Doppler shifts are output from the receiver whereas expected Doppler shifts can be computed from the relative receiver–satellite motion.

3.1 Observed Doppler shifts

A Doppler shift is a by–product of the signal tracking done by the receiver (Xu, 2003), p. 38. As will be seen in section 4.3, the noise level of the observed Doppler shift is too high for detecting small cycle slips.

3.2 Expected Doppler shifts

As mentioned, the Doppler shift is the relative receiver–satellite velocity vector projected onto the line of sight from the receiver to the satellite divided by the transmitted wavelength. Therefore, when the position vectors and the velocity vectors of the receiver and the satellite are known, the Doppler shift is estimated using the dot–product.

$$\Delta f = \left(\frac{\mathbf{r}_r - \mathbf{r}^s}{\|\mathbf{r}_r - \mathbf{r}^s\|} \bullet (\mathbf{v}_r - \mathbf{v}^s) \right) \frac{1}{\lambda}, \tag{8}$$

- ▷ where $\mathbf{r}_r$ and $\mathbf{r}^s$ are the position vectors of the receiver and the satellite,
- ▷ $\mathbf{v}_r$ and $\mathbf{v}^s$ are the the velocity vectors of the receiver and the satellite, and
- ▷ λ is the wavelength of the transmitted signal.

As mentioned in section 2, the precision of the predicted double differenced carrier phase observation depends on the precision of the Doppler shift. Assuming that all the elements in the position vectors and in the velocity vector are independent (which they are not), error propagation of equation (8) shows that the precision of the expected Doppler shift is very sensitive to errors in the velocity vectors and not so sensitive to errors in the position vectors. This is illustrated in section 5 and section 6.

Before estimating the Doppler shift using equation (8), the position vectors and the velocity vectors of the receiver and the satellite need to be computed. The position vectors and the velocity vectors are expressed in WGS84.

3.2.1 Satellite position and velocity

The satellite position vector can be computed from the broadcast ephemeris and the algorithm given in (Global Positioning Systems Directorate, 2011), p. 103. The position vector has an accuracy of less than two metres, (University of New Brunswick, Department of Geodesy and Geomatics Engineering, GPS Lab, 2012), (International GNSS Service (IGS), 2012).

The satellite velocity vector can be computed from the broadcast ephemeris and the algorithms described in (Remondi, 2004) and (Zhang et al., 2006). The accuracy of the velocity vector is at the millimetres per second level (Remondi, 2004), p. 183, (Zhang et al., 2006), p. 294, (van Diggelen, 2009), p. 49.

3.2.2 Receiver position and velocity

The receiver position vector and velocity vector can be estimated with several techniques. Here, two techniques are outlined. One technique is to estimate the receiver position vector and velocity vector separately from each other from code observations and Doppler shift observations. The position vector along with the receiver clock bias are estimated from code observations as described in (Misra and Enge, 2001), pp. 176–181. The velocity vector along with the receiver clock

drift are estimated from Doppler shift observations as described in (Misra and Enge, 2001), pp. 196–197. Estimating the velocity vector and the clock drift from Doppler shift observations is closely related to estimating the position vector and the clock bias from code measurements as the geometry matrix relating the observations and the unknowns is the same in both cases (Misra and Enge, 2001), pp. 196–197. Using this technique, the receiver position vector and velocity vector are estimated each epoch independently of the neighbouring epochs. With SA off, the position typically has an accuracy of a few metres per axis. Again, with SA off, an accuracy of 0.2 m/s per axis (95%) is achievable for velocities estimated from Doppler shifts (United States Coast Guard, 1996), p. 3.7.

Another technique for estimating the receiver position vector and velocity vector is to use code observations and an 8–state extended Kalman filter as described in (Brown and Hwang, 2012), pp. 318–330. This filter estimates the receiver position vector and velocity vector along with the receiver clock bias and clock drift. Because of the recursive nature of the Kalman filter, the estimated position vector and velocity vector at one epoch depend on the previous epochs.

For this case study, it is chosen to estimate the receiver position vector and velocity vector using the former of the two techniques outlined above.

4 Experiment

Carrier phase observations, code observations, and Doppler shift observations were collected to illustrate the use of expected Doppler shift observations for identifying cycle slips. The observations were collected near Aalborg University, Denmark, April 25, 2012. In addition, these observations were collected in both static and kinematic mode. Two identical low–cost single frequency ublox ANTARIS 4 LEA-4T evaluation kits were used for collecting the observations. The ublox receivers cost approximately € 300 apiece when they were bought in 2008. The half-cycle carrier phase observations were collected at 1 Hz frequency using *u–center*, which among other things is a serial data collection software provided by ublox. The collected observations were converted to RINEX observation files using TEQC (UNAVCO, 2012). TEQC was also used for screening the observations for cycle slips. No cycle slips were identified by TEQC in the observations presented in this article. A RINEX broadcast ephemeris file was downloaded from the CDDIS GNSS archive (NASA, 2012). In both the static and the kinematic experiment PRN 8 was chosen as reference satellite, when the double differenced observations were computed. Furthermore, in both experiments the master receiver was fixed to the roof of one of the university buildings with a clear view of the sky.

4.1 Static experiment

The rover receiver was in turn placed 40 metres from the master receiver and 5 kilometres from the master receiver. In both locations the rover receiver had a

clear view of the sky, while observations were collected for 300 seconds.

4.2 Kinematic experiment

During the kinematic experiment the rover receiver was mounted on the top of a car. Observations were collected for 150 seconds while the car drove on a public road with a clear view of the sky at distances between 150 metres to 1050 metres from the master receiver, see Figure 1.

Figure 1. *Trajectory from kinematic experiment. The master receiver is marked with a black dot in the lower left corner.*

4.3 Noise level in collected Doppler shift observations

Figure 2 illustrates the noise level in the collected Doppler shift observations in the static experiment with only 40 metres separation between the master receiver and the rover receiver. The figure shows the deviations (ΔDD) between observed double differenced carrier phase observations and predicted double differenced carrier phase observations for four satellites. The predicted double differenced carrier phase observations are computed using equation (6) and the actual Doppler shift observations collected with the ublox receivers.The noise level of the double differenced carrier phase observations is a few millimetres (Cederholm, 2010). Therefore, the variations shown in Figure 2 are caused by the collected Doppler shift observations. This indicates that the collected Doppler shift observations are not usable for detecting small cycle slips. The reference satellite (PRN8) has a minimum elevation angle of 56° during the 300 seconds time span. During the same time span, the four other satellites (PRN5, PRN10, PRN13, PRN26) have minimum elevation angles of 55°, 49°, 34°, and 21°, respectively. The deviations from these four satellites are presented in the figure, as they represent the satellites in the data set well. Deviations from other satellites being illustrated in later figures are chosen for the same reason.

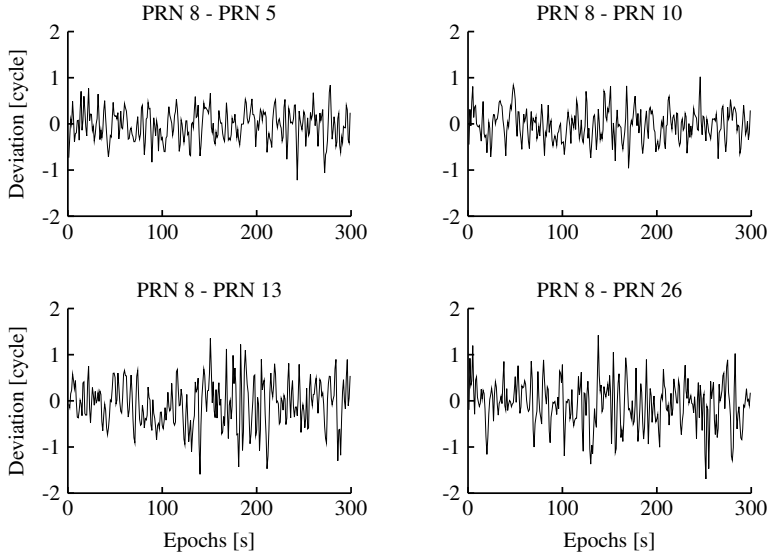

Figure 2. *Static experiment. Deviations between observed double differenced carrier phase observations and predicted double differenced carrier phase observations computed from observed Doppler shifts. The two GPS receivers are 40 metres apart.*

5 Results of static and kinematic experiments

In both the static and the kinematic experiment, the position vector of the master receiver is known in advance, and the velocity vector of the master receiver is obviously zero. The position vector and velocity vector of the satellites are computed as outlined in section 3.2.1. All predicted double differenced carrier phase observations are computed with equation (6). The Doppler shift observations that enter into equation (6) are all computed with equation (8). The figures in this section show differences between observed double differenced carrier phase observations and predicted double differenced carrier phase observations for selected satellites.

5.1 Static experiment

Figure 3 shows the differences in the static experiment with 5 kilometres separation between the two receivers. The rover receiver velocity vector is zero as the receiver is static. The rover receiver position vector is computed as the mean of 300 epoch–by–epoch estimates of the position; each estimate is computed from code observations as outlined in section 3.2.2. The figure reveals that the noise level of the differences is less that one tenth of a cycle.

Two artificial cycle slips of ± 0.5 cycle have been inserted into the raw collected carrier phase observations from the rover receiver. The two artificial cycle slips are inserted at epochs 100 and 200. Furthermore, the two artificial cycle slips are inserted into the carrier phase observations from all satellites in the rover receiver data set. No artificial cycle slips have been inserted into the carrier phase observations from the master receiver. Figure 4 shows that the cycle slips are ea-

sily detected. Apart from the artificial cycle slips, Figure 4 is identical to Figure 3.

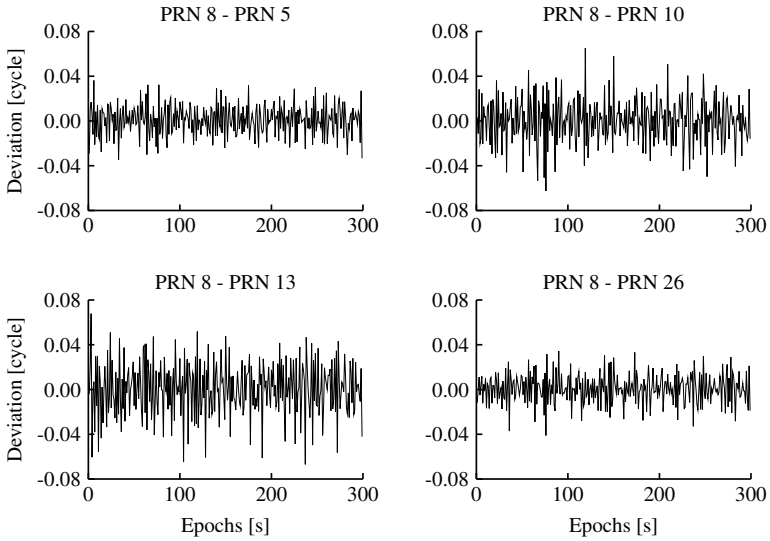

Figure 3. *Static experiment. Deviations between observed double differenced carrier phase observations and predicted double differenced carrier phase observations computed from expected Doppler shifts. The two GPS receivers are 5 kilometres apart.*

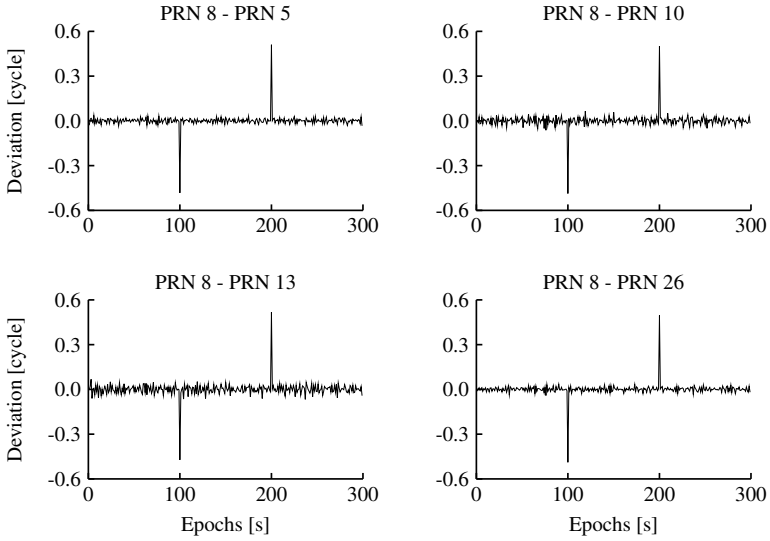

Figure 4. *Static experiment. Deviations between observed double differenced carrier phase observations and predicted double differenced carrier phase observations computed from expected Doppler shifts. Two artificial cycle slips of* ± 0.5 *cycle have been inserted at epochs 100 and 200. The two GPS receivers are 5 kilometres apart.*

5.2 Kinematic experiment

Figure 5 shows the differences between the observed double differenced carrier phase observations and the predicted double differenced carrier phase observations while the car is driving along the trajectory shown in Figure 1. The rover receiver position vector and the rover receiver velocity vector are both estimated using the epoch–by–epoch technique outlined in section 3.2.2. The noise level in the figure makes it impossible to identify small cycle slips. One reason for this is that the accuracies of the estimated positions and/or velocities are too low. The dynamics of the car and the sampling interval may also be reasons for the less efficient cycle slip detection.

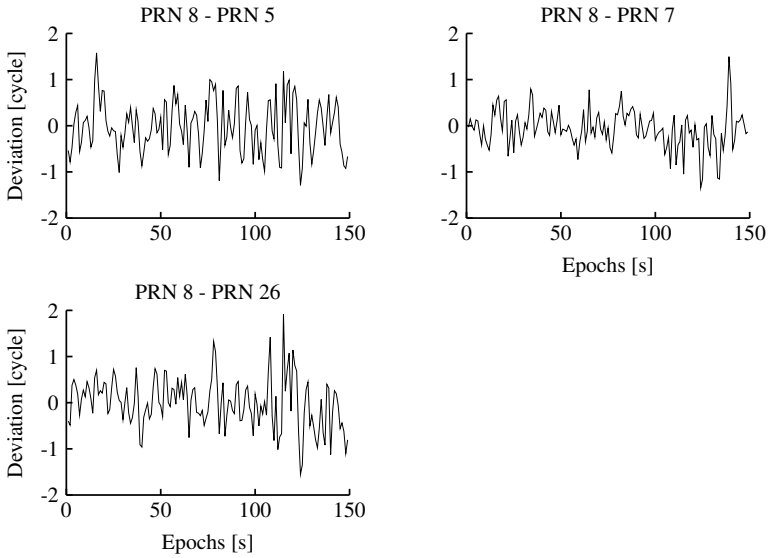

Figure 5. *Kinematic experiment. Deviations between observed double differenced carrier phase observations and predicted double differenced carrier phase observations computed from expected Doppler shifts. Both the rover receiver position vector and the velocity vector are estimated epoch–by–epoch.*

6 Impact of position and velocity noise on predicted double differenced carrier phase observations

It is apparent from section 5.2 that the noise level of the rover receiver velocity vector and/or position vector is too high for detecting 0.5 cycle slips in the kinematic experiment. Likewise, it is mentioned in section 3.2 that the precision of the expected Doppler shift is very sensitive to errors in the velocity vectors and not so sensitive to errors in the position vectors. This section illustrates the effects of the position and velocity noise on the predicted double differenced carrier phase observations. The section is based on data from the static experiment which, however, is treated as a kinematic data set. By using data from the static experiment rather than data from the kinematic experiment the uncertainties caused by the car

dynamics are left out. This implies that the findings of this section are probably overly optimistic compared to findings based on a kinematic data set.

First, it is shown in section 6.1 how the noise of the rover position vector and the noise of the rover velocity vector estimated from the static data set effect the predicted double differenced carrier phase observations. Next, it is examined in section 6.2 how low the noise level of the rover receiver position vector and velocity vector should be in order to safely detect cycle slips of 0.5 cycle.

The findings in this section are solely based on a data set spanning 300 seconds. Therefore, it should be realized that the findings are not conclusive at all. The findings only provide a snapshot of the sensitivity of the proposed cycle slip detection technique in one location on the Earth at one moment in time. Variations in the relative receiver–satellite geometry are very small during the time span. Further, section 6.2 is based on simulations and computer generated white gaussian noise that represent the noise of the rover receiver position vector and rover receiver velocity vector. The computer generated white gaussian noise does not truly reflect a real life scenario as the precision of the rover receiver position vector and rover receiver velocity vector also depends on the relative receiver–satellite geometry.

6.1 Separation of position and velocity noise

Predicted double differenced carrier phase observations are computed twice from the static data set to visualize the effects of position noise and velocity noise, respectively. The effects are illustrated in Figure 6 and Figure 8. Figure 6 shows the effects of velocity noise whereas Figure 8 shows the effects of position noise.

In Figure 6, the uncertainty of the rover receiver position vector is minimized by computing the rover position as the mean of 300 epoch–by–epoch estimates of the position. The rover receiver velocity vector is estimated epoch–by–epoch from the collected Doppler shift observations as outlined in section 3.2.2. Figure 7 shows the estimated epoch–by–epoch rover velocities that are used for producing Figure 6. The standard deviations of the estimated velocities are close to 0.1 m/s along all three coordinate axes.

In Figure 8, the rover receiver position vector is computed epoch–by–epoch and the rover receiver velocity vector is zero. Figure 9 shows how the estimated epoch–by–epoch coordinates that are used for producing Figure 8 deviate from the mean coordinates. The standard deviations of the estimated coordinates are less than 1 m along all three coordinate axes.

It is apparent that the two artificial cycle slips are easily detected in Figure 8 whereas they cannot be detected in Figure 6. The two figures illustrate that the predicted double differenced carrier phase observations are much more sensitive to errors in the rover receiver velocity vector than it is to errors in the rover receiver position vector.

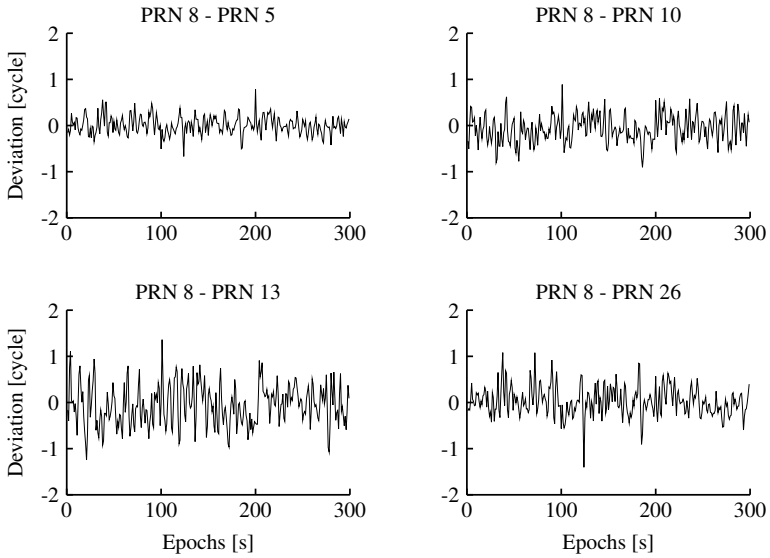

Figure 6. *Static experiment. Deviations between observed double differenced carrier phase observations and predicted double differenced carrier phase observations computed from expected Doppler shifts. The rover receiver position vector is the mean of 300 epoch–by–epoch position estimates. The rover receiver velocity vector is estimated epoch–by–epoch. Two artificial cycle slips of* ± 0.5 *cycle have been inserted at epochs 100 and 200. The two GPS receivers are 5 kilometres apart.*

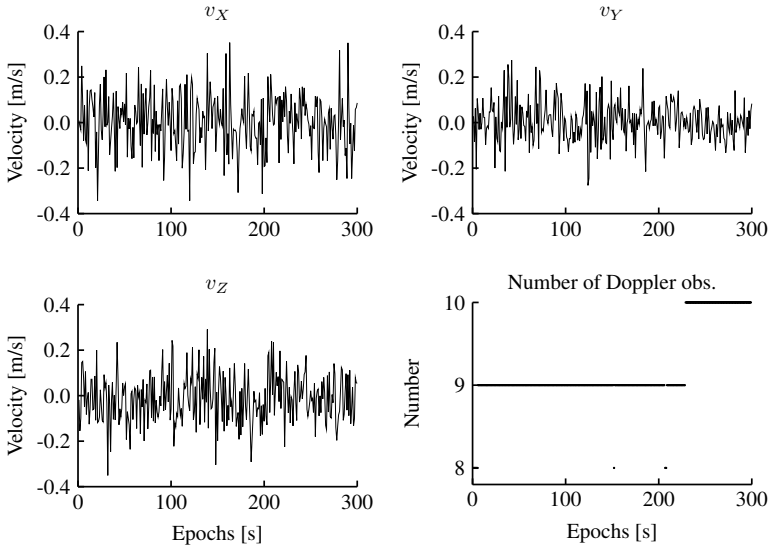

Figure 7. *Static experiment. Rover receiver velocity estimated from observed Doppler shift. Number of observations used in estimation.*

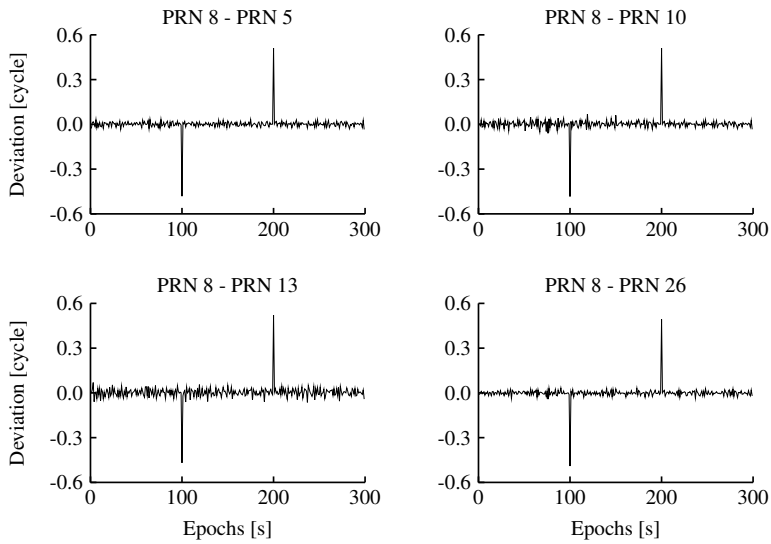

Figure 8. *Static experiment. Deviations between observed double differenced carrier phase observations and predicted double differenced carrier phase observations computed from expected Doppler shifts. The rover receiver position vector is estimated epoch–by–epoch. The rover receiver velocity vector is zero. Two artificial cycle slips of* ± 0.5 *cycle have been inserted at epochs 100 and 200. The two GPS receivers are 5 kilometres apart.*

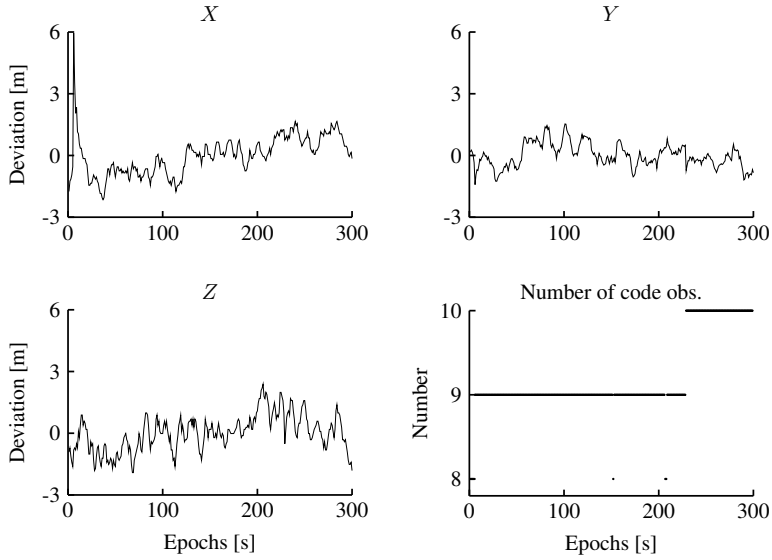

Figure 9. *Static experiment. Deviations of rover receiver position from mean position. The positions are estimated from code observations. Number of observations used in estimation.*

6.2 Position and velocity accuracies necessary for detecting 0.5 cycle slips

In order to safely identify cycle slips of 0.5 cycle, the standard deviation of the difference between the observed double differenced carrier phase observation and the predicted double differenced carrier phase observation needs to be significantly smaller than 0.5 cycle. Assuming that the differences are normally distributed, a standard deviation of the differences ($\sigma_{\Delta DD}$) of $1/3$ of 0.5 cycle implies that only $1/370 \approx 0.3\%$ of the deviations exceeds 0.5 cycle. Likewise, a standard deviation of the differences of $1/4$ of 0.5 cycle implies that only $1/15787 \approx 0.006\%$ of the deviations exceeds 0.5 cycle. Several simulations using the static data set and computer generated white gaussian noise representing the noise of the rover receiver position vector and rover receiver velocity vector are carried out to estimate which position and velocity accuracies are needed to safely identify 0.5 cycle slips. The computer generated white gaussian noise representing the noise of the rover receiver position vector is named σ_{XYZ}. Likewise, the computer generated white gaussian noise representing the noise of the rover receiver velocity vector is named σ_{vXvYvZ}. Both σ_{XYZ} and σ_{vXvYvZ} represent the noise along each coordinate axis. Like in section 6.1, the effects of position noise and velocity noise are examined separately.

First, the effects of the uncertainties in the rover receiver position vector are assessed. The static data set spans 300 epochs. For all epochs, the mean of the 300 epoch–by–epoch estimates of the position is used as the rover position. White gaussian noise (σ_{XYZ}) is added to the mean position. The rover receiver velocity vector is zero and no noise is added to the velocity vector. Based on the rover receiver position vector and the rover receiver velocity vector, the expected Doppler shift and the predicted double differenced carrier phase observations are computed for each epoch using equations (8) and (6). The predicted double differenced carrier phase observations are subtracted from the observed double differenced carrier phase observations, and the standard deviation of these differences ($\sigma_{\Delta DD}$) is computed. These calculations are repeated several times. In each run the magnitude of the added white gaussian noise is altered. Table 1 shows corresponding values of added white gaussian noise (σ_{XYZ}) and the standard deviations ($\sigma_{\Delta DD}$) resulting from the simulations. Table 1 indicates that $\sigma_{\Delta DD}$ is virtually insensitive to the uncertainties of the rover receiver position. Added noise with a standard deviation of 1 m which corresponds to the actual noise level of the computed epoch–by–epoch positions (see Figure 9) does not affect $\sigma_{\Delta DD}$ at all.

Next, the effects of the uncertainties in the rover receiver velocity vector is assessed. The standard deviation of the rover receiver position vector computed epoch–by–epoch is less than 1 m along all three coordinate axes (see section 6.1). As a noise level of this magnitude does not affect $\sigma_{\Delta DD}$ the rover receiver epoch–by–epoch positions are used in the simulation. The rover receiver velocity vector is set to zero with added white gaussian noise (σ_{vXvYvZ}). Again, several simulations are computed each with different magnitudes of added white gaussian noise. In each simulation, the standard deviation of the differences between the observed

and the predicted double differenced carrier phase observations is computed. Table 2 shows that $\sigma_{\Delta DD}$ is very sensitive to uncertainties in the rover receiver velocity vector. Added noise with a standard deviation of 0.1 m which corresponds to the actual noise level of the computed epoch–by–epoch velocities (see Figure 7) results in a $\sigma_{\Delta DD}$ of approximately one third of a cycle which is double the standard deviation needed to safely identify 0.5 cycle slips.

Table 1. *Computer generated white gaussian rover position noise (σ_{XYZ}) and standard deviation of differences between observed and predicted double differenced carrier phases ($\sigma_{\Delta DD}$). Velocity noise $\sigma_{vXvYvZ} = 0$ m/s.*

σ_{XYZ} [m]	$\sigma_{\Delta DD}$ [cycle]
0	0.02
1	0.02
10	0.02
50	0.04
100	0.08
150	$0.13 \approx 1/8$
200	$0.17 \approx 1/6$

Table 2. *Computer generated white gaussian rover velocity noise (σ_{vXvYvZ}) and standard deviation of differences between observed and predicted double differenced carrier phases ($\sigma_{\Delta DD}$). Position noise $\sigma_{XYZ} \approx 1$ m.*

σ_{vXvYvZ} [m/s]	$\sigma_{\Delta DD}$ [cycle]
0.00	0.02
0.01	0.04
0.02	0.07
0.03	0.10
0.04	$0.13 \approx 1/8$
0.05	$0.17 \approx 1/6$
0.10	0.33

7 Conclusions and future work

The article presents a case study of the applicability of using expected Doppler shifts for identifying cycle slips in double differenced carrier phase observations collected with two GPS receivers.

Doppler shifts can be used for predicting double differenced carrier phase observations from one epoch to the next. The case study is based on observations collected with two low–cost single frequency ublox ANTARIS 4 LEA-4T GPS receivers. The noise level of the collected Doppler shifts is too high for identifying small cycle slips. Instead of detecting cycle slips using the collected Doppler shift, the article attempts to use expected Doppler shifts for identifying cycle slips. Once the positions and the velocities of the satellites and the two GPS receivers are known, the expected Doppler shift can be computed and used for cycle slip detection. The positions and the velocities of the satellites are computed from the broadcast ephemerides. The positions and the velocities of the GPS receivers are computed from collected code observations and collected Doppler shift observations.

Two experiments are carried out. In one experiment the two GPS receivers are

static while collecting observations. In the other experiment one receiver is static and the other is mounted on a moving car while observations are being collected.

In the static experiment the positions of the receiver are computed from the collected code observations, and the velocities are zero as the receivers do not move. In this case, cycle slips with a magnitude of 0.5 cycle are easily identified.

In the kinematic experiment, the positions of the receiver are computed from the collected code observations, and the velocities are computed from the collected Doppler shift observations. In this case, cycle slips can only be identified if they have a magnitude of several cycles. The smaller efficiency in the kinematic experiment compared to the static experiment is caused by the poor accuracy of the velocities being estimated from the collected Doppler shift observations.

Simulations indicate that the standard deviation of the velocities should be less than $0.05 m/s$ to safely detect 0.5 cycle slips. Therefore, the performance in the kinematic case may be improved if the accuracy of the velocity of the moving receiver is improved. In future work, this accuracy may be improved by means of introducing additional sensors, by using other estimation techniques, or by increasing the sampling frequency.

Acknowledgements. Financial support to this research by *Det Obelske Familiefond* (*The Obel Family Foundation*) is gratefully acknowledged. Birthe Nørskov, Aalborg University, is thanked for improving the English language. Anders Otte, Aalborg University, is thanked for assisting with the data collection.

References

Brown, R. G. and Hwang, P. Y. (2012). Introduction to Random Signals and Applied Kalman Filtering with Matlab Exercises. John Wiley & Sons, Inc., 4 edition.

Cannon, M. E., Schwarz, K. P., Wei, M., and Delikaraoglou, D. (1992). A consistency test of airborne GPS using multiple monitor stations. Journal of Geodesy, 66:2–11.

Cederholm, P. (2010). Statistical characteristics of L1 carrier phase observations from four low-cost GPS receivers. Nordic Journal of Surveying and Real Estate Research, 7(1):58–75.

Global Positioning Systems Directorate (2011). IS-GPS-200 Navstar GPS Space Segment/Navigation User Segment Interfaces. Technical report, Global Positioning Systems Directorate.

Hofmann-Wellenhof, B., Lichtenegger, H., and Wasle, E. (2008). GNSS - Global Navigation Satellite Systems GPS, GLONASS, Galileo & more. Springer-Verlag, 1 edition.

International GNSS Service (IGS) (2012). IGS Products. `http://igscb.jpl.nasa.gov/components/prods.html`.

Lipp, A. and Gu, X. (1994). Cycle-Slip Detection and Repair in Integrated Navigation Systems. In Position Location and Navigation Symposium, pages 681–688. IEEE.

Liu, Z. (2010). A new automated cycle slip detection and repair method for a single dual-frequency GPS receiver. Journal of Geodesy, 85(3):171–183.

Mertikas, S. P. and Rizos, C. (1997). On-line detection of abrupt changes in the carrier-phase measurements of GPS. Journal of Geodesy, 71:469–482.

Misra, P. and Enge, P. (2001). Global Positioning System: Signals, Measurements, and Performance. Ganga-Jamuna Press.

NASA (2012). CDDIS - NASA's Archive of Space Geodesy Data. `http://cddis.nasa.gov/gnss_datasum.html`.

Remondi, B. W. (2004). Computing satellite velocity using the broadcast ephemeris. GPS Solutions, 8:181–183.

UNAVCO (2012). TEQC - The Toolkit for GPS/GLONASS/Galileo/SBAS Data. `http://facility.unavco.org/software/teqc/teqc.html`.

United States Coast Guard (1996). NAVSTAR GPS User Equipment Introduction. Technical report, United States Coast Guard Navigation Center.

University of New Brunswick, Department of Geodesy and Geomatics Engineering, GPS Lab (2012). GPS broadcast orbit accuracy statistics. `http://gge.unb.ca/gauss/htdocs/grads/orbit/`.

van Diggelen, F. (2009). A-GPS: Assisted GPS, GNSS, and SBAS. Artech House.

Xu, G. (2003). GPS Theory, Algorithms and Applications. Springer.

Zhang, J., Zhang, K., Grenfell, R., and Deakin, R. (2006). GPS Satellite Velocity and Acceleration Determination using the Broadcast Ephemeris. Journal of Navigation, 59:293–305.